JOURNAL OF SOLID STATE CHEMISTRY 93, 9–16 (1991)

Structure and Properties of Hopeites $(Mg_xZn_{1-x})_3(PO_4)_2 \cdot 4H_2O$

S. HAUSSÜHL, B. MIDDENDORF, AND M. DÖRFFEL

Institut für Kristallographie der Universität zu Köln, Zülpicher Str. 49, 5000 Köln 1, West-Germany

Received August 23, 1990; in revised form December 21, 1990

Mg-hopeites $(Mg_xZn_{1-x})_3(PO_4)_2 \cdot 4H_2O$ were prepared by crystallization from hot aqueous solutions (70°C). The structure of $(Mg_{0.206}Zn_{0.794})_3(PO_4)_2 \cdot 4H_2O$ has been determined from 1612 unique reflections (Mo$K\alpha$, $R = 0.033$): *Pnma*, $a_1 = 10.594(2)$, $a_2 = 18.333(2)$, $a_3 = 5.029(2)$Å, $Z = 4$, $D_{calc} = 2.943$ g cm^{-3}. The structure resembles that of pure hopeite. However, the magnesium atoms occupy only the six-coordinated site. The thermal behavior of hopeites is strongly influenced by the substitution of Zn by Mg. The dehydration range is shifted to higher temperatures with increasing Mg content. A strongly anisotropic thermal expansion was measured by X-ray diffraction in a temperature range of −40° to 50°C. Experiments to substitute Zn by Ca, Sr, and Ba in the hopeite failed. A hitherto unknown monoclinic phase with the composition $BaZn_2(PO_4)_2 \cdot H_2O$ and $a_1 = 4.707(2)$, $a_2 = 7.840(2)$, $a_3 = 8.061(3)$Å, and $\alpha_2 = 88.99(4)°$ was found.

Introduction

Zinc phosphating is widely used in industrial surface pretreatments for the painting of metals. Pure hopeite, $Zn_3(PO_4)_2 \cdot 4H_2O$, is formed during phosphating treatments of galvanized steels in solutions containing zinc as the major metallic component. The phosphate layer formed on the metal undergoes different attacks, i.e., a thermal one during paint baking and a chemical one during cathodic electrodeposition of paint coating.

Recently Arnaud *et al.* (*1*), Roland and Gottwald (*2*), and Kent and Petschel (*3*) reported on manganese and/or nickel incorporation in the hopeite coating. They claimed that such polycationic conversion coatings improve the resistance against alkaline and thermal attacks. The aim of this report is to investigate the properties of mixed crystals of hopeite in which Zn is substituted by bivalent earth alkaline ions.

Experimental

Synthesis and Chemical Analysis

Stoichiometric mixtures of various compositions were prepared according to Eq. (1).

$$3xMg(NO_3)_2 + 3(1-x)Zn(NO_3)_2 + 2H_3PO_4 + 4H_2O \xrightarrow{pH\,5} (Mg_xZn_{1-x})_3(PO_4)_2 \cdot 4H_2O + 6HNO_3 \quad (1)$$

Since the hopeites are soluble in excess acid, their precipitation required a controlled addition of alkali ions. The filtered and dried precipitates were identified by X-ray powder diffraction.

For the growth of single crystals a precipitate obtained from a solution of disodium hydrogen orthophosphate and nitrates of zinc and magnesium was dissolved by adding nitric acid. Crystals formed upon adding a diluted solution of ammonium or sodium

0022-4596/91 $3.00

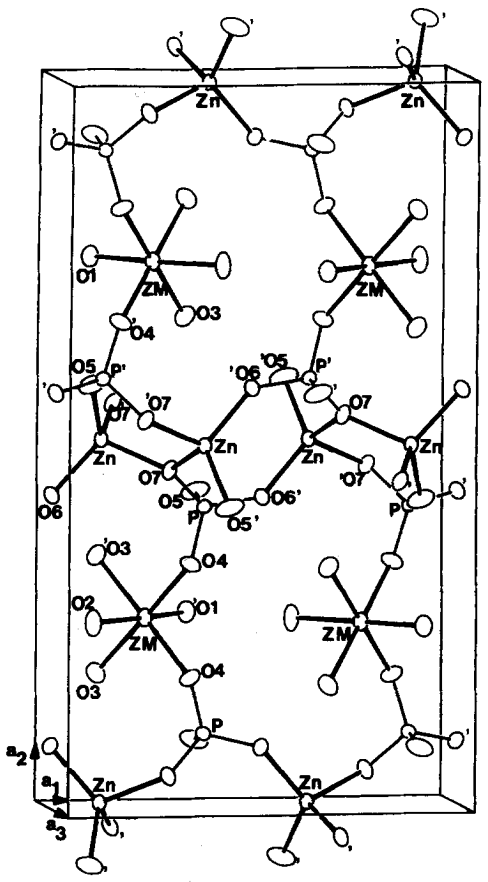

FIG. 1. ORTEP-plot of the hopeite crystal structure. Atoms outside the unit cell are labeled with a superscript prime.

hydroxide. These crystals with dimensions up to 2 mm are colorless. They show orthorhombic–dipyramidial symmetry with the following forms: {010}, {110}, {230}, and {011}. The composition of the powder and the crystals was analyzed by atomic absorption spectroscopy and wet-chemical procedures.

In order to prove the existence of hopeites in which Zn is substituted by Ca, Sr, and Ba, syntheses analogous to those of Mg-hopeite were tried. For calcium we obtained in addition to pure hopeite the well-known phases scholzite, $CaZn_2(PO_4)_2 \cdot nH_2O$, and brushite, $CaHPO_4 \cdot 2H_2O$ (*4–10*). If the molar ratio of Zn and Ca in the solutions is larger than 2 : 3, we find hopeite and scholzite as reaction products. For the calcium-rich case the deposited phases are scholzite and brushite.

It was also impossible to replace zinc by strontium in the hopeite structure. In a wide concentration range we get a jelly-like, X-ray amorphous precipitate. If the ratio of Zn and Sr is less than 1 : 4 we obtain a powder which could be analyzed as α-$SrHPO_4$.

Barium with the largest ionic radius (1.33 Å) (*11*) formed a new phase, $BaZn_2(PO_4)_2 \cdot H_2O$, which is not identical with other barium–zinc phosphates known in the system $BaO–ZnO–P_2O_5$ (*12*). TGA analyses show a decrease in the weight of the sample by 3.8 wt% at about 300°C, which corresponds to one molecule of water in the structure.

Single crystals of $BaZn_2(PO_4)_2 \cdot H_2O$ could be grown by slow evaporation of aqueous solutions (90°C). The pseudohexagonal plates (diameter up to 10 mm, thickness about 0.05 mm) are built up from six sectors. Microscopic inspections showed the optical character to be biaxial negative with an angle $2V$ of about 27°. The X-ray powder diffractograms could be indexed with a monoclinic metric: $a_1 = 4.707(2)$, $a_2 = 7.840(2)$, $a_3 = 8.061(3)$Å; $\alpha_2 = 88.99(4)°$.

Laue and Buerger precession photographs revealed the Laue group $2/m$ and the absence of systematic extinctions. No second harmonic generation could be detected which suggests the existence of an inversion center. Experiments to synthesize mixed crystals of the type $Ba(Mg_xZn_{1-x})_2(PO_4)_2 \cdot H_2O$ failed. Therefore, we assume that zinc occupies a tetrahedral site in $BaZn_2(PO_4)_2 \cdot H_2O$.

From our results it can be concluded that Ca, Sr, and Ba ions are too large to fit into the hopeite structure.

Dehydration

The dehydration of Mg-hopeites was examined by thermal gravimetric analysis

TABLE I

DATA COLLECTION AND REFINEMENT PARAMETERS

Substance	$(Mg_{0.206}Zn_{0.794})_3(PO_4)_2 * 4H_2O$
Formula weight	432.76
Space group	*Pnma*
a_1 (Å)	10.594(2)
a_2 (Å)	18.333(2)
a_3 (Å)	5.029(2)
D_{calc} (g cm^{-3}) ($Z = 4$)	2.943
μ (Mo$K\alpha$) (cm^{-1})	63.97
θ min, max (deg)	1.0–35.0
Scan-mode	$\omega - 2\theta$
Min/max h,k,l	h(0/17); k(0/29); l(0/8)
Total data	2575
Total unique data ($I \geq 3\sigma(I)$)	1612
No. of parameters	92
Extinction parameter E	$6.14\ 10^{-7}$
$F_{corr} = F_c/(1 + E \cdot F_c^2 \cdot Lp)$	0.91
Max residual electron density (eÅ^{-3})	0.033; 0.057
Final R; R_w	

(TGA) (heating from 20 to 570°C at a rate of 10°C min^{-1}) and differential scanning calorimetry (DSC).

The DSC measurements were carried out in a dry nitrogen atmosphere at temperatures between 60 and 220°C. The heating rate was 2°C min^{-1}.

Thermal Expansion

The temperature-induced shift of the lattice constants was determined by X-ray powder diffraction from the variation of θ angles of 52 reflections in a temperature range of $-40°$ to 50°C ($\theta_{max} = 31°$). The coefficients of thermal expansion α_{ii} resulted from a computer-aided least-squares fit of the θ-values, where a correction of the displacement (s) from the rotation axis ($\Delta\theta_s = -(s/l) \cdot \cos\theta$; l = camera radius) was included.

Structure Analysis

The crystal structure of hopeite, $Zn_3(PO_4)_2 \cdot 4H_2O$, has already been reported by Liebau (*13*), Kawahara *et al.* (*14*), Whitaker (*15*) and Hill and Jones (*16*).

For our structure analysis we used a crystal of the composition $(Mg_{0.206}Zn_{0.794})_3(PO_4)_2 \cdot 4H_2O$ with the dimensions 0.3 × 0.2 × 0.2 mm. The data collection was carried out on an Enraf–Nonius CAD4 diffractometer. The unit cell was determined from 25 well-centered reflections in the angular range $12° < \theta < 15°$. Details of the subsequent data collection and refinement are given in Table I. An empirical absorption correction, based on the ψ-scan of six reflections, was used, together with corrections for Lorentz and polarization effects. The centrosymmetric space group *Pnma* was determined from systematic extinctions and the absence of a second harmonic generation effect (Nd-YAG laser; wavelength, 1064 nm).

For the first least-squares refinement the atomic coordinates of P and O reported by Hill and Jones (*17*) were used. The Zn and Mg atoms were located from Fourier synthesis. Refinement with anisotropic temperature factors converged at a final R value of 0.033. In order to prove the chemical composition and the distribution of magnesium in the structure we calculated R values for various ratios of zinc and magnesium. The refinements converged to a minimum of $R = 0.033$, if magnesium occupies only the octahedral site and if the composition of the crystal corresponds to the result of the chemical analysis (see above).

The sites of the hydrogen atoms could not be resolved. Atomic and thermal parameters are given in Table II and Table III.

Results and Discussion

Description of the Structure

In natural hopeite the Zn atoms are divided in the ratio 2 : 1 between one half of the tetrahedral sites (Zn) and one quarter of the octahedral sites. The other tetrahedral positions are occupied by P, while the remaining octahedra are vacant. Figure 1 shows the hopeite crystal structure. The octahedral sites which contain zinc and magnesium are labeled "ZM" (ZM = 0.62 Mg + 0.38 Zn).

TABLE II

ATOMIC COORDINATES AND ISOTROPIC THERMAL PARAMETERS OF THE ATOMS

Atom	x	y	z	U_{eq}(Å^2)
ZM[a]	0.26247(7)	0.250	0.0729(2)	0.0186(2)
Zn	0.14241(3)	0.49897(2)	0.20834(7)	0.0124(1)
P	0.39693(6)	0.40469(4)	0.2270(1)	0.0111(1)
O(1), H_2O	0.1065(3)	0.750	0.2581(7)	0.0223(8)
O(2), H_2O	0.1145(3)	0.250	0.3450(8)	0.0273(8)
O(3), H_2O	0.3361(2)	0.6700(1)	0.3394(6)	0.0257(6)
O(4)	0.3591(2)	0.3273(3)	0.2820(4)	0.0196(5)
O(5)	0.0997(3)	0.5792(1)	0.4305(5)	0.0268(5)
O(6)	0.0253(2)	0.4218(1)	0.1415(5)	0.0203(5)
O(7)	0.3009(2)	0.4597(1)	0.3619(4)	0.0156(5)

Note. Equivalent isotropic U is defined as one-third of the trace of the U_{ij} tensor; standard deviations in parentheses.

[a] ZM: 0.62 Mg + 0.38 Zn.

The ZMO_6 octahedra are built up from four water molecules (O(1), O(2) and 2*O(3)), and two oxygen atoms (O(4)) which are shared with two PO_4 tetrahedra, thus forming the complex $ZMO_2(H_2O)_4$. Each PO_4 tetrahedron shares one corner with a ZMO_6 octahedron and three corners with different ZnO_4 tetrahedra. The ZnO_4 tetrahedra are connected by two PO_4 tetrahedra (O(5)–O(6)) and by two corners with different PO_4 and ZnO_4 tetrahedra (O(7)). Therefore, the oxygen atom O(7) is involved in three polyhedra, one PO_4 and two ZnO_4.

The calculations of the Mg-hopeite have shown that the Mg-atoms occupy only the octahedral ZM positions. Contrary to Hill and Jones (*16*) we did not find a deficiency of atoms (Zn and Mg, see above) on the octahedral site.

This is consistent with the observation that it is impossible to obtain crystals which contain more than one magnesium atom per

TABLE III

THERMAL PARAMETERS [Å^2], DEFINED BY THE TEMPERATURE FACTOR $T = \exp\{-2\pi^2\Sigma_{ij}U_{ij}h_ih_j \cdot a^*_ia^*_j\}$; STANDARD DEVIATIONS IN PARENTHESES

Atom	U_{11}	U_{22}	U_{33}	U_{12}	U_{13}	U_{23}
ZM[a]	0.0174(3)	0.0214(3)	0.0170(3)	0	−0.0006(3)	0
Zn	0.0124(1)	0.0133(1)	0.0115(2)	−0.0003(1)	0.0002(1)	−0.0008(1)
P	0.0141(3)	0.0088(2)	0.0103(2)	0.0007(2)	−0.0006(2)	0.0005(2)
O(1)	0.019(1)	0.030(2)	0.018(1)	0	−0.004(1)	0
O(2)	0.017(1)	0.043(2)	0.022(1)	0	0.005(1)	0
O(3)	0.027(1)	0.021(1)	0.029(1)	0.0075(9)	0.006(1)	0.001(1)
O(4)	0.030(1)	0.0114(8)	0.0173(9)	−0.0062(8)	−0.0093(8)	0.0021(7)
O(5)	0.051(1)	0.0167(9)	0.0126(9)	0.011(1)	−0.004(1)	−0.0039(8)
O(6)	0.0124(7)	0.0156(8)	0.033(1)	−0.0025(7)	0.0038(9)	−0.0046(9)
O(7)	0.0133(7)	0.0207(9)	0.0129(8)	0.0049(7)	−0.0025(7)	−0.0038(8)

[a] ZM: 0.62 Mg + 0.38 Zn.

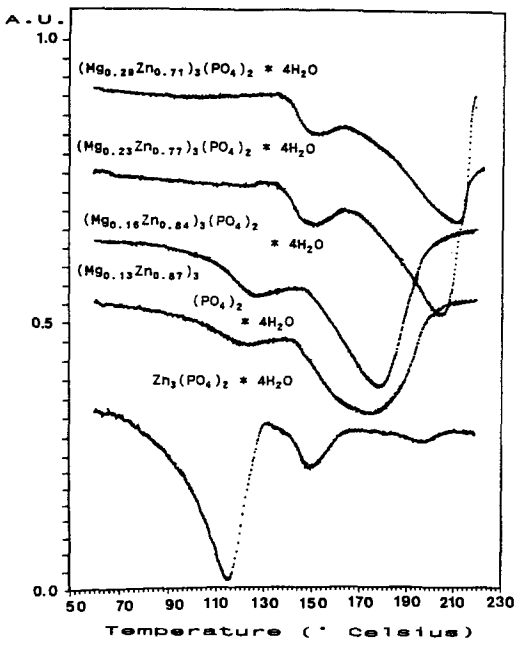

FIG. 2. DSC curves of pure and Mg-hopeites.

formula unit. All X-ray powder diffraction patterns of Mg-hopeite yielded nearly the same *d* values and only slightly different intensities. Precipitates which contain more than 33.3 mol% magnesium are X-ray amorphous.

Bond angles and distances for the PO_4^- and ZnO_4 tetrahedra reported by Hill and Jones (*16*) are basically identical to those found in this study (Table V). The mean value obtained for the P–O bond (1.537(13)Å) corresponds to the results on other orthophosphates. An examination of the individual distances and angles indicates that the tetrahedra are distorted, both in bond lengths and in bond angles. The oxygen atom O(7) which is involved in three polyhedra (see Fig. 1) shows the largest bond distances from the central atoms P and Zn, respectively. Also for the ZnO_4 tetrahedron we observed a significant distortion with bond distances between 1.901(2) and 1.993(2) Å. All distances in the ZMO_6 octahedron are shorter than those in pure hopeite.

Thermal Properties

Dehydration of pure and Mg-hopeites. In all DSC runs we observed endothermal processes. Furthermore, we found a decrease of density with a rise of temperature.

The TGA data of pure hopeite, $Zn_3(PO_4)_2 \cdot 4H_2O$, show that the dehydration takes three steps, each one corresponding to the release of an integer number of water molecules per formula unit. The first dehydration starts at 68°C and by the time the temperature reaches 132°C, two molecules of water have been lost (one molecule of water = 3.93 wt%). This involves a transformation from hopeite to the monoclinic dihydrate (*17*) with the formula $Zn_3(PO_4)_2 \cdot 2H_2O$ (Fig. 2).

In the temperature range of 135 to 166°C the dihydrate loses weight corresponding to one molecule of water. The dehydration of the last molecule of water starts at 290°C and involves a transformation to the anhydrous salt (Fig. 3).

From the dehydration experiments it became obvious that the Mg-hopeites also contain four molecules of water. The dehydration of these Mg-hopeites is different from the pure hopeite. Up to a temperature of 210°C three molecules of water are lost steadily. The dehydration of the last molecule of water starts at about 315°C. The results of the thermal analyses are presented in Figs. 2 and 3: the larger the magnesium content, the higher the dehdyration temperature of the samples. The higher dehydration temperature of Mg-hopeite layers might improve the stability of anticorrosive coatings of baking varnishes. Experiments under industrial conditions are in progress.

Contrary to recently published conclusions (*17*) our results show that the dehydration process occurs in three and two steps, each with a loss of an integer number of water molecules per formula unit (Fig. 3).

TABLE IV

Mg-HOPEITE INTERATOMIC DISTANCES (Å), WITH e.s.d.'s IN PARENTHESES IN TERMS OF THE LAST DIGIT

PO_4-tetrahedron		ZnO_4-tetrahedron	
P— O(4)	1.517(2)	Zn — O(5)	1.901(2)
— O(5)i	1.517(2)	— O(6)	1.911(2)
— O(6)ii	1.541(2)	— O(7)	1.984(2)
— O(7)	1.573(2)	— O(7)i	1.993(2)
O(5) — O(7)	2.514(3)	O(5) — O(7)	3.129(3)
— O(4)	2.505(4)	— O(7)i	3.129(3)
— O(6)ii	2.527(3)	— O(6)	3.167(4)
O(7) — O(4)	2.535(3)	O(7) — O(7)i	3.109(3)
— O(6)ii	2.477(3)	— O(6)	3.176(3)
O(4) — O(6)ii	2.500(3)	O(7)i — O(6)	3.176(3)

$ZMO_2(H_2O)_4$-octahedron		Authors' data[a]	Data after HILL & JONES[b]
ZM— O(4)	(2)	2.035(2)	2.046(3)
— O(1)iii		2.098(3)	2.099(4)
— O(2)		2.089(4)	2.102(4)
— O(3)iii	(2)	2.155(3)	2.171(3)
O(3)i — O(3)iii		2.934(4)	2.949(6)
— O(1)iii	(2)	2.870(4)	2.879(4)
— O(4)	(2)	3.038(3)	3.066(4)
— O(2)	(2)	2.934(4)	3.008(5)
O(1)iii — O(4)	(2)	2.807(4)	3.024(4)
O(4) — O(4)iv		2.836(3)	2.840(5)
— O(2)	(2)	2.971(4)	2.982(4)

Note. Symmetry transformations for atoms outside the asymmetric unit: i: $\frac{1}{2} - x$, $1 - y$, $z - \frac{1}{2}$; ii: $\frac{1}{2} + x$, y, $\frac{1}{2} - z$; iii: $\frac{1}{2} - x$, $y - \frac{1}{2}$, $z - \frac{1}{2}$; iv: x, $\frac{1}{2} - y$, z.

[a] octahedral site containing 62% magnesium and 38% zinc

[b] octahedral site containing zinc

We think that the differences in the dehydration behavior, especially the higher thermal stability of the magnesium hopeites, result from the stronger interaction of the Mg ion with the water molecules in the octahedron complex $ZMO_2(H_2O)_4$, as suggested by the shorter Mg–O distances compared to the Zn–O distances (Table IV). The reason for the different water losses in the first and second step leading to different stable intermediate phases (dihydrate, monohydrate) is not yet clear. The final dehydrated products of pure zinc hopeite and magnesium hopeite show different X-ray powder diagrams. The full dehydration of pure hopeite at about 600°C yielded $Zn_3(PO_4)_2$, a phase described by the ASTM card 11-0035, whereas a powder of $(Mg_{0.26}Zn_{0.74})_3(PO_4)_2 \cdot 4H_2O$ heated at 600°C, produces a diffraction pattern corresponding to $MgZn_2(PO_4)_2$ (ASTM card 31-1468). The formula $MgZn_2(PO_4)_2$ was confirmed by wet chemical analyses.

Rehydration processes. The rehydration of pure hopeites and of those containing magnesium was accomplished after 21 days at 20°C and at a relative humidity of 95%. Diffractograms of the samples were recorded after different intervals. We found

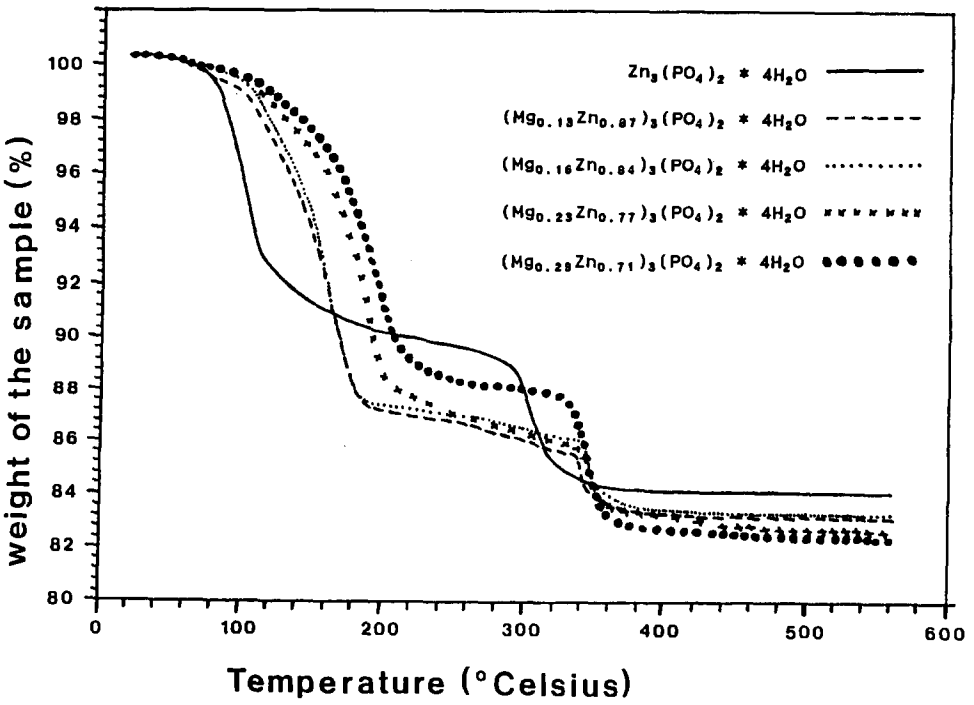

FIG. 3. TGA curves of pure and Mg-hopeites.

that after 6 days already 75% of the dehydrated hopeite had returned to its original crystal structure. After 14 days, more than 95% of the dehydrated sample was rehydrated to hopeite.

Thermal Expansion

We observed a pronounced anisotropic behavior of thermal expansion. The expansion parallel to the a_3 axis is nearly 20 times larger than along the a_2 direction. Furthermore, the thermal expansion parallel to the a_1 and a_2 axes show almost equal absolute values. For pure hopeite we found the coefficients of thermal expansion $\alpha_{11} = -1(3)$, $\alpha_{22} = 1(2)$, and $\alpha_{33} = 31(3) \cdot 10^{-6}\ K^{-1}$. An increasing content of magnesium affects α_{33} in a linear proportion yielding, e.g., $\alpha_{33} = 24(3) \cdot 10^{-6}K^{-1}$ for a powder with the composition $(Mg_{0.25}Zn_{0.75})_3(PO_4)_2 \cdot 4H_2O$. Within the estimated standard deviation the thermal expansion of the a_1 and a_2 axes is unchanged.

TABLE V

Mg-HOPEITE INTERATOMIC ANGLES (°), WITH e.s.d.'s IN PARENTHESES IN TERMS OF THE LAST DIGIT

PO_4-tetrahedron		Zn-tetrahedron	
O(5)i–P–O(7)	108.9(1)	O(5)–Zn–O(7)	104.7(1)
–O(4)	111.0(1)	–O(7)i	106.92(9)
–(6)ii	111.5(2)	–O(6)	121.4(1)
O(7)–P–O(4)	110.3(1)	O(7)–Zn–O(7)i	102.92(8)
–O(6)ii	105.4(1)	–O(6)	110.42(9)
O(4)–P–O(6)ii	109.7(1)	O(7)i–Zn–O(6)	108.9(1)

$ZMO_2(H_2O)_4$-octahedron

O(3)i –ZM–O(3)iii	85.8(1)	
–O(1)iii	84.9(1)	(2)
–O(4)	92.92(9)	(2)
–O(2)	89.3(1)	(2)
O(1)iii–ZM–O(4)	93.61(9)	(2)
O(4) –ZM–O(4)iv	88.31(9)	
–O(2)	92.2(1)	(2)
O(1)iii–ZM–O(2)	172.0(1)	
O(4) –ZM–O(3)iii	178.(1)	(2)

Note. For symmetry code see footnote to Table IV.

An interpretation of the heavily anisotropic thermal expansion will be given in a forthcoming paper on physical properties of hopeites (*18*).

Acknowledgments

The authors thank Drs. Elsässer, Endres and Seidel for critical and helpful comments. We are also indebted to the Henkel KGaA, Düsseldorf, for financial support.

References

1. Y. ARNAUD, E. SAKAKIAN, J. LENOIR, AND M. ROCHE, *Appl. Surf. Sci.* **32,** 296 (1988).
2. W. A. ROLAND AND K. H. GOTTWALD, *Metalloberfläche* **42,** 301 (1988).
3. G. D. KENT AND M. PETSCHEL, *Prod. Finish.* **56** (1988).
4. R. J. HILL AND A. R. MILNES, *Mineral. Mag.* **39,** 684 (1974).
5. B. D. STURMAN, R. C. ROUSE, AND P. J. DUNN, *Amer. Mineral.* **66,** 843 (1981).
6. R. J. HILL, J. E. JOHNSON, AND J. B. JONES, *N. Jb. Miner. Mh.* **1,** 1 (1978).
7. A. R. MILNES AND R. J. HILL, *N. Jb. Miner. Mh.* **1,** 25 (1977).
8. K. H. TAXER, *Amer. Mineral.* **60,** 1019 (1975).
9. C. A. BEEVERS, *Acta. Crystallogr.* **11,** 273 (1958).
10. N. A. CURRY AND D. W. JONES, *J. Chem. Soc. A.*, 3725 (1971).
11. R. D. SHANNON, *Acta. Crystallogr. Sect. A* **32,** 751 (1976).
12. M. V. HOFFMAN, *J. Electrochem. Soc.* **110**(12), 1223 (1963).
13. F. LIEBAU, *Acta. Crystallogr.* **18,** 352 (1965).
14. A. KAWAHARA, Y. TAKANO AND M. TAKAHASHI, *Mineral. J. (Japan)* **7,** 289 (1973).
15. A. WHITAKER, *Acta. Crystallogr. Sect. B* **51,** 2026 (1975).
16. R. J. HILL AND J. B. JONES, *Amer. Mineral.* **61,** 987 (1976).
17. Y. ARNAUD, E. SAHAKIAN, AND M. ROMAND, *Appl. Surf. Sci.* **32,** 281 (1988).
18. M. FRIEDRICH AND S. HAUSSÜHL (1990), to be published.